Chapter 8

Fundamental Analysis for Visible Light Communication with Input-Dependent Noise

Jin-Yuan Wang, Jun-Bo Wang and Yongjin Wang

Additional information is available at the end of the chapter

http://dx.doi.org/10.5772/68019

Abstract

Recently, visible light communication (VLC) has drawn much attention. In literature, the noise in VLC is often assumed to be independent of the input signal. This assumption neglects a fundamental issue of VLC: due to the random nature of photon emission in the lighting source, the strength of the noise depends on the signal itself. Therefore, the input-dependent noise in VLC should be considered. Given this, the fundamental analysis for the VLC with input-dependent noise is presented in this chapter. Based on the information theory, the theoretical expression of the mutual information is derived. However, the expression of the mutual information is not in a closed form. Furthermore, the lower bound of the mutual information is derived in a closed form. Moreover, the theoretical expression of the bit error rate is also derived. Numerical results verify the accuracy of the derived theoretical expressions in this chapter.

Keywords: visible light communication, input-dependent noise, mutual information, bit error rate

1. Introduction

As one of the emerging optical wireless communication techniques, the visible light communication (VLC) has drawn considerable attention recently from both the academy and industry [1–3]. Compared to the traditional radio frequency (RF) wireless communication, VLC has many advantages, such as freedom from hazardous electromagnetic radiation, no licensing requirements, low-cost frontends, large spectrum bandwidth (as shown in **Figure 1**), large channel capacity, and so on. In VLC, both illumination and communication are simultaneously implemented. Moreover, the transmitted optical signal is non-negative. Therefore, the developed theory and analysis results in traditional RF wireless communication are not directly applicable to VLC.

Up to now, the research on VLC can be divided into two categories: the demo system design and theoretical analysis. As research continues, a variety of demo platforms arise. **Table 1** shows the development of the VLC demo systems. As can be seen in **Table 1**, the transmit rate of the VLC system increases from several Mbps to several Gbps in the last decade, which indicates that the VLC has attractive prospects of development. Specifically, the transmit rates of the early demo systems are low, but the transmit distances are long and the data are processed in real time. With the development of communication techniques, more and more

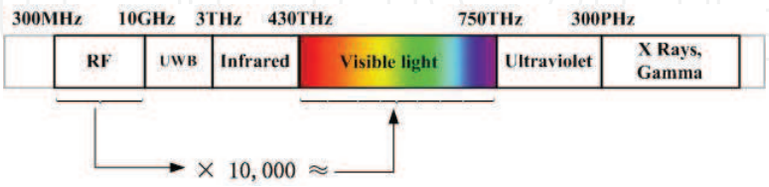

Figure 1. The electromagnetic spectrum.

Time (year)	Research & Development Group	Transmit rate (bit/s)	Transmit distance (m)	Data processing mode	
				Offline	Online
2000	Keio University, Japan	10 M	5	√	
2002	Keio University, Japan	87 M	1.65	√	
2008	Taiyo Yuden Co., Ltd, Japan	100 M	0.2	√	
	Jinan University, China	4 M	2.5	√	
2009	University of Oxford, UK, et al.	100 M	0.1	√	
	Heinrich Hertz Institute, Germany	125 M	5		√
2011	Heinrich Hertz Institute, Germany	803 M	0.12		√
2012	Kinki University, Japan	614 M			√
	National Chiao Tung University, Taiwan	1.1 G	0.23		√
	Santa Ana school for Advanced Studies, Italy	3.4 G	0.3		√
2013	University of Strathclyde, UK	1.5 G			√
	National Chiao Tung University, Taiwan	3.22 G	0.25		√
	The University of Edinburgh, UK	10 G			√
	Southeast University, China	480 M	3	√	
2014	Fudan University, China	3.25 G			√
2015	Pknuyong National University, Korea	3 G	2.15		√
	The PLA Information Engineering University, China	50 G			√

Table 1. The development of the VLC demo systems.

VLC testbeds with high transmit rates are developed successfully, but the real-time processing becomes very hard. Therefore, more advanced processing techniques are needed for VLC.

In the aspect of theoretical analysis, much work has been done on VLC. In Ref. [4], the channel capacity for VLC using inverse source coding is investigated. However, the theoretical expression of the capacity is not presented. Under the non-negative and average optical intensity constraints, the closed expression of capacity bounds is derived in Ref. [5]. Based on Ref. [5], a tight upper bound on the capacity is derived in Ref. [6]. By adding a peak optical intensity constraint, tight capacity bounds are further derived in Ref. [7]. In Ref. [8], the capacity bounds for multiple-input-multiple-output VLC are derived. In Ref. [9], the capacity and outage probability for the parallel optical wireless channels are analysed. Furthermore, low signal-to-noise ratio (SNR) capacity for the parallel optical wireless channels is obtained in Ref. [10]. It should be noted that the noises in Refs. [4–10] are all assumed to be independent with the input signal. This assumption is reasonable if the ambient light is strong or if the receiver suffers from intensive thermal noise. However, in practical VLC systems, typical illumination scenarios offer very high SNR [11, 12]. For high power, this assumption neglects a fundamental issue of VLC: due to the random nature of photon emission in the light emitting diode (LED), the strength of noise depends on the signal itself [13]. Up to now, the performance of the VLC with input-dependent noise has not been discussed completely.

In this chapter, we consider a VLC system with input-dependent Gaussian noise and investigate the fundamental performance of the VLC system. The main contributions of this chapter are given as follows:

1. A channel model with input-dependent Gaussian noise for the VLC is considered. In existing literature, the noise is generally assumed to be independent of the signal. However, this assumption is not applicable to the VLC system in some cases. In this chapter, a more general channel model is established which is corrupted by an additive Gaussian noise, however, with noise variance depending on the signal itself.

2. The mutual information of the VLC system is analysed. Based on the channel model, the exact expression of the mutual information is derived. However, the exact expression of the mutual information is not in a closed form. After that, a closed-form expression of the lower bound on the mutual information is derived.

3. The bit error rate (BER) of the VLC system is obtained. By employing the on-off keying (OOK), the theoretical expression of the BER for the VLC system is derived. Moreover, some asymptotic behaviour for the BER is also presented.

4. To show the accuracy of the derived theoretical expressions, the theoretical results are thoroughly confirmed by Monte-Carlo simulations.

The remainder of this chapter is organized as follows. The system model is described in Section 2. Section 3 presents the exact expression and the lower bound of the mutual information. In Section 4, the theoretical expression of the BER is derived. Numerical results are given in Section 5 before conclusions are drawn in Section 6.

2. System model

Consider a point-to-point VLC system, as shown in **Figure 2**. At the transmitter, an LED is employed as the lighting source, which performs the electrical-to-optical conversion. Then, the optical signal is propagated through the VLC channel. At the receiver, a PIN photodiode (PD) is used to perform the optical-to-electrical conversion. To amplify the derived electrical signal, a high impedance amplifier is employed. In this chapter, the main noise sources include thermal noise, shot noise and amplifier noise. The thermal noise and the amplifier noise are independent of the signal, and each of the two noise sources can be well modelled by Gaussian distribution [14]. Although its distribution can also be assumed to be Gaussian, the strength of the shot noise depends on the signal itself. Mathematically, the received electrical signal Y at the receiver can be written as [13]

$$Y = rGX + \sqrt{rGX}Z_1 + Z_0 \tag{1}$$

where r denotes the optoelectronic conversion factor of the PD. $Z_0 \sim N(0, \sigma^2)$ denotes the input-independent Gaussian noise. $Z_1 \sim N(0, \varsigma^2\sigma^2)$ denotes the input-dependent Gaussian noise, where $\varsigma^2 \geq 0$ denotes the ratio of the input-dependent noise variance to the input-independent noise variance. Z_0 and Z_1 are independent with each other.

In Eq. (1), G denotes the channel gain between the LED and the PD, which can be expressed as [15]

$$G = \frac{(m+1)A}{2\pi d^2} \cos^m(\varphi) T(\psi) g(\psi) \cos(\psi) \tag{2}$$

where m denotes the order of the Lambertian emission, A is the physical area of the PD and d, φ and ψ are the distance, the angle of irradiance and the angle of incidence from the LED to the PD, respectively. $T(\psi)$ is the gain of an optical filter and $g(\psi)$ is the gain of an optical concentrator.

Note that the channel gain in Eq. (2) is a constant, where the positions of the LED and the PD are given. Moreover, r in Eq. (1) is a constant for a fixed PD. Without loss of generality, the values of both G and r are set to be one. Therefore, Eq. (1) can be simplified as [16]

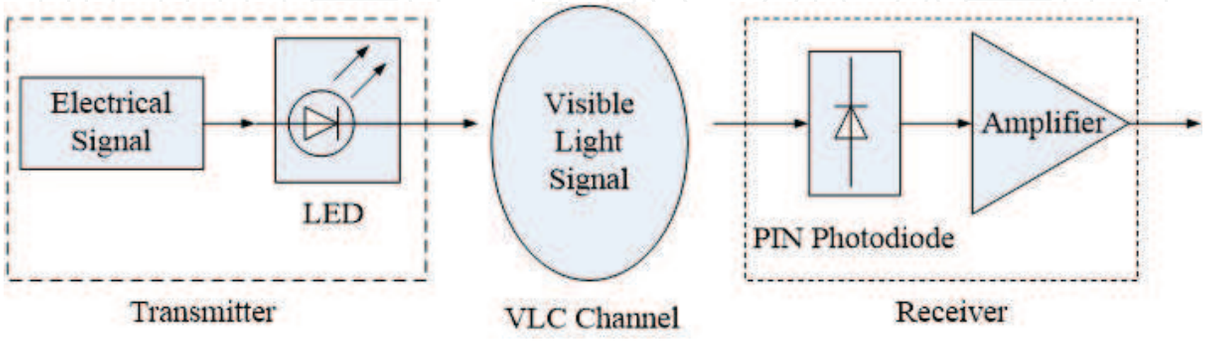

Figure 2. The point-to-point VLC system.

$$Y = X + \underbrace{\sqrt{X}Z_1 + Z_0}_{\triangleq Z}. \tag{3}$$

In VLC, information is transmitted by modulating the instantaneous optical intensity [17], and thus, X should be non-negative, that is,

$$X \geq 0. \tag{4}$$

Due to the eye and skin safety regulations, the peak optical intensity of the LED is limited [17], that is,

$$X \leq A \tag{5}$$

where A is the peak optical intensity of the LED.

Considering the illumination requirement in VLC, the average optical intensity cannot be changed but can be adjusted according to the users' requirement (dimming target) [18]. Therefore, the average optical intensity constraint is given by

$$E(X) = \xi P \tag{6}$$

where $E(\cdot)$ denotes the expectation operator and $\xi \in (0, 1]$ denotes the dimming target. $P \leq A$ is the normal optical intensity of the LED.

3. Mutual information analysis

Mutual information is an important performance indicator for wireless communication systems. In this section, the exact expression of the mutual information and the closed-form expression of the lower bound on the mutual information for the VLC will be derived, respectively.

3.1. Exact expression of mutual information

Assume that N-ary intensity modulation is employed. Let $X \in \{x_1, x_2, \cdots, x_N\}$ be the optical intensity symbol drawn from the equiprobable modulation constellation, that is,

$$\Pr(X = x_i) = \frac{1}{N}. \tag{7}$$

According to Eq. (3), the conditional probability density function (PDF) of Y when given $X = x_i$ can be written as [19]

$$f_{Y|X}(y|x_i) = \frac{1}{\sqrt{2\pi(1 + x_i\varsigma^2)}\sigma} \exp\left(-\frac{(y - x_i)^2}{2(1 + x_i\varsigma^2)\sigma^2}\right). \tag{8}$$

Furthermore, the PDF of Y can be expressed as

$$\begin{aligned} f_Y(y) &= \sum_{i=1}^{N} \Pr(X = x_i) f_{Y|X}(y|x_i) \\ &= \frac{1}{N} \sum_{i=1}^{N} \frac{1}{\sqrt{2\pi(1 + x_i\varsigma^2)}\sigma} \exp\left(-\frac{(y - x_i)^2}{2(1 + x_i\varsigma^2)\sigma^2} \right). \end{aligned} \tag{9}$$

The mutual information between X and Y is given by

$$\begin{aligned} I(X;Y) &= H(X) - H(X|Y) \\ &= \sum_{i=1}^{N} \frac{1}{N} \log_2 N - \sum_{i=1}^{N} \int_{-\infty}^{\infty} \frac{1}{N} f_{Y|X}(y|x_i) \log_2 \left(\frac{f_Y(y)}{\Pr(X = x_i) f_{Y|X}(y|x_i)} \right) \mathrm{d}y \\ &= \log_2 N - \frac{1}{N} \sum_{i=1}^{N} \int_{-\infty}^{\infty} \frac{\exp\left(-\frac{(y - x_i)^2}{2(1 + x_i\varsigma^2)\sigma^2} \right)}{\sqrt{2\pi(1 + x_i\varsigma^2)}\sigma} \log_2 \underbrace{\left(\frac{\sum_{t=1}^{N} \frac{\exp\left(-\frac{(y - x_t)^2}{2(1 + x_t\varsigma^2)\sigma^2} \right)}{\sqrt{2\pi(1 + x_t\varsigma^2)}\sigma}}{\frac{\exp\left(-\frac{(y - x_i)^2}{2(1 + x_i\varsigma^2)\sigma^2} \right)}{\sqrt{2\pi(1 + x_i\varsigma^2)}\sigma}} \right)}_{\triangleq I_1} \mathrm{d}y \end{aligned} \tag{10}$$

where $H(\cdot)$ denotes the entropy.

From Eq. (3), we have $Z = Y - X$. Therefore, let $z = y - x_i$, and thus, I_1 in Eq. (10) can be further written as

$$\begin{aligned} I_1 &= \int_{-\infty}^{\infty} \frac{\exp\left(-\frac{z^2}{2(1 + x_i\varsigma^2)\sigma^2} \right)}{\sqrt{2\pi(1 + x_i\varsigma^2)}\sigma} \log_2 \left[\frac{\sum_{t=1}^{N} \frac{\exp\left(-\frac{(z + x_i - x_t)^2}{2(1 + x_t\varsigma^2)\sigma^2} \right)}{\sqrt{2\pi(1 + x_t\varsigma^2)}\sigma}}{\frac{\exp\left(-\frac{z^2}{2(1 + x_i\varsigma^2)\sigma^2} \right)}{\sqrt{2\pi(1 + x_i\varsigma^2)}\sigma}} \right] \mathrm{d}y \\ &= E_Z \left\{ \log_2 \left[\frac{\sum_{t=1}^{N} \frac{\exp\left(-\frac{(z + x_i - x_t)^2}{2(1 + x_t\varsigma^2)\sigma^2} \right)}{\sqrt{2\pi(1 + x_t\varsigma^2)}\sigma}}{\frac{\exp\left(-\frac{z^2}{2(1 + x_i\varsigma^2)\sigma^2} \right)}{\sqrt{2\pi(1 + x_i\varsigma^2)}\sigma}} \right] \right\} \\ &= E_Z \left\{ \log_2 \left[\sum_{t=1}^{N} \frac{\sqrt{1 + x_i\varsigma^2}}{\sqrt{1 + x_t\varsigma^2}} \exp\left(\frac{z^2}{2(1 + x_i\varsigma^2)\sigma^2} - \frac{(z + x_i - x_t)^2}{2(1 + x_t\varsigma^2)\sigma^2} \right) \right] \right\} \end{aligned} \tag{11}$$

Therefore, Eq. (10) can be further written as

$$I(X;Y)=\log_2 N-\frac{1}{N}\sum_{i=1}^{N}E_Z\left\{\log_2\left[1+\sum_{\substack{t=1\\t\neq i}}^{N}\frac{\sqrt{1+x_i\varsigma^2}}{\sqrt{1+x_t\varsigma^2}}\exp\left(\frac{z^2}{2(1+x_i\varsigma^2)\sigma^2}-\frac{(z+x_i-x_t)^2}{2(1+x_t\varsigma^2)\sigma^2}\right)\right]\right\} \tag{12}$$

Remark 1: Let the average SNR be $\gamma=\xi P/[(1+\xi P\varsigma^2)\sigma^2]$. Because ξ, P and ς are non-negative and finite numbers, $\gamma\to\infty$ (or 0) is equivalent to $\sigma^2\to 0$ (or ∞). Apparently, $I(X;Y)$ in Eq. (12) is a monotonic increasing function with respect to γ. Therefore, we have

$$\lim_{\gamma\to\infty}I(X;Y)=\log_2 N \tag{13}$$

which indicates that the maximum value of $I(X;Y)$ is $\log_2 N$.

Moreover, we have

$$\lim_{\gamma\to 0}I(X;Y)=\log_2 N-\frac{1}{N}\sum_{i=1}^{N}\log_2\left(1+\sum_{\substack{t=1\\t\neq i}}^{N}\frac{\sqrt{1+x_i\varsigma^2}}{\sqrt{1+x_t\varsigma^2}}\right) \tag{14}$$

Remark 2: When $\varsigma=0$, Eq. (3) reduces to $Y=X+Z_0$. Therefore, the mutual information can be simplified as

$$I(X;Y)|_{\varsigma=0}=\log_2 N-\frac{1}{N}\sum_{i=1}^{N}E_Z\left\{\log_2\left[1+\sum_{\substack{t=1\\t\neq i}}^{N}\exp\left(\frac{z^2-(z+x_i-x_t)^2}{2\sigma^2}\right)\right]\right\} \tag{15}$$

3.2. Lower bound on mutual information

It should be noted that it is very hard to derive a closed-form expression of Eq. (12). In this subsection, a lower bound on the mutual information will be derived.

To facilitate the description, Eq. (12) can be further expressed as

$$\begin{aligned}I(X;Y)=\log_2 N&-\frac{1}{N}\sum_{i=1}^{N}\underbrace{E_Z\left\{\log_2\left[\exp\left(\frac{z^2}{2(1+x_i\varsigma^2)\sigma^2}\right)\right]\right\}}_{I_2}\\&\underbrace{-\frac{1}{N}\sum_{i=1}^{N}E_Z\left\{\log_2\left[\sum_{t=1}^{N}\frac{\sqrt{1+x_i\varsigma^2}}{\sqrt{1+x_t\varsigma^2}}\exp\left(-\frac{(z+x_i-x_t)^2}{2(1+x_t\varsigma^2)\sigma^2}\right)\right]\right\}}_{I_3}\end{aligned} \tag{16}$$

For I_2 in Eq. (16), we have

$$\begin{aligned} I_2 &= \frac{\log_2(e)}{2(1+x_i\varsigma^2)\sigma^2}\int_{-\infty}^{+\infty} z^2 \frac{\exp\left(-\frac{z^2}{2(1+x_i\varsigma^2)\sigma^2}\right)}{\sqrt{2\pi(1+x_i\varsigma^2)\sigma^2}}\mathrm{d}z \\ &= \frac{\log_2(e)}{2(1+x_i\varsigma^2)\sigma^2}(1+x_i\varsigma^2)\sigma^2 \\ &= \frac{1}{2}\log_2(e). \end{aligned} \tag{17}$$

Using the Jensen's inequality for concave function, an upper bound of I_3 in Eq. (16) can be written as

$$\begin{aligned} I_3 &= E_Z\left\{\log_2\left[\sum_{t=1}^{N}\frac{\sqrt{1+x_i\varsigma^2}}{\sqrt{1+x_t\varsigma^2}}\exp\left(-\frac{(z+x_i-x_t)^2}{2(1+x_t\varsigma^2)\sigma^2}\right)\right]\right\} \\ &\le \log_2\left\{\sum_{t=1}^{N}\frac{\sqrt{1+x_i\varsigma^2}}{\sqrt{1+x_t\varsigma^2}}E_Z\left[\exp\left(-\frac{(z+x_i-x_t)^2}{2(1+x_t\varsigma^2)\sigma^2}\right)\right]\right\} \\ &= \log_2\left\{\sum_{t=1}^{N}\frac{\sqrt{1+x_i\varsigma^2}}{\sqrt{1+x_t\varsigma^2}}\int_{-\infty}^{+\infty}\frac{\exp\left(-\frac{(z+x_i-x_t)^2+z^2}{2(1+x_t\varsigma^2)\sigma^2}\right)}{\sqrt{2\pi(1+x_t\varsigma^2)\sigma^2}}\mathrm{d}z\right\} \\ &= \log_2\left(\sum_{t=1}^{N}\frac{\sqrt{1+x_i\varsigma^2}}{\sqrt{2(1+x_t\varsigma^2)}}\exp\left(-\frac{(x_i-x_t)^2}{4(1+x_t\varsigma^2)\sigma^2}\right)\right). \end{aligned} \tag{18}$$

Substituting Eqs. (17) and (18) into Eq. (16), a lower bound of $I(X;Y)$ can be derived as

$$\begin{aligned} I_{\mathrm{Low}}(X;Y) &= \log_2 N - \frac{1}{2}\log_2(e) + \frac{1}{2} \\ &- \frac{1}{N}\sum_{i=1}^{N}\log_2\left(1+\sum_{\substack{t=1\\t\neq i}}^{N}\frac{\sqrt{1+x_i\varsigma^2}}{\sqrt{1+x_t\varsigma^2}}\exp\left(-\frac{(x_i-x_t)^2}{4(1+x_t\varsigma^2)\sigma^2}\right)\right). \end{aligned} \tag{19}$$

Remark 3: Obviously, $I_{\mathrm{Low}}(X;Y)$ in Eq. (19) is a monotonic increasing function with respect to γ. Therefore, we have

$$\lim_{\gamma\to\infty} I_{\mathrm{Low}}(X;Y) = \log_2 N - \frac{1}{2}\log_2(e) + \frac{1}{2} \tag{20}$$

which indicates that the maximum value of $I_{\mathrm{Low}}(X;Y)$ is $\log_2 N - \log_2(e)/2 - 1/2$.

Moreover, we have

$$\lim_{\gamma\to 0} I_{\mathrm{Low}}(X;Y) = \log_2 N - \frac{1}{2}\log_2(e) + \frac{1}{2} - \frac{1}{N}\sum_{i=1}^{N}\log_2\left(1+\sum_{\substack{t=1\\t\neq i}}^{N}\frac{\sqrt{1+x_i\varsigma^2}}{\sqrt{1+x_t\varsigma^2}}\right) \tag{21}$$

Remark 4: According to Eqs. (13) and (20), we have

$$\lim_{\gamma\to\infty} I(X;Y) - \lim_{\gamma\to\infty} I_{\text{Low}}(X;Y) = \frac{1}{2}[\log_2(e) - 1]. \tag{22}$$

Similarly, from Eqs. (14) and (21), we have

$$\lim_{\gamma\to 0} I(X;Y) - \lim_{\gamma\to 0} I_{\text{Low}}(X;Y) = \frac{1}{2}[\log_2(e) - 1]. \tag{23}$$

From Eqs. (22) and (23), it can be concluded that a constant performance gap $[\log_2(e) - 1]/2$ exists between $I(X;Y)$ and $I_{\text{Low}}(X;Y)$ at low and high SNR regions.

Remark 5: When $\varsigma = 0$, $I_{\text{Low}}(X;Y)$ can be simplified as

$$\begin{aligned} I_{\text{Low}}(X;Y)|_{\varsigma=0} &= \log_2 N - \frac{1}{2}\log_2(e) + \frac{1}{2} \\ &- \frac{1}{N}\sum_{i=1}^{N}\log_2\left(1 + \sum_{\substack{t=1 \\ t\neq i}}^{N}\exp\left(-\frac{(x_i - x_t)^2}{4\sigma^2}\right)\right). \end{aligned} \tag{24}$$

4. BER analysis

In this section, the BER of the VLC with input-dependent noise is analysed. To facilitate the analysis, OOK is employed as the modulation scheme. Suppose that the transmitted optical signal is drawn equiprobably from the OOK constellation and $2\xi P \le A$ always holds, we have

$$X \in \{0, 2\xi P\}. \tag{25}$$

Therefore, the BER for the VLC with OOK can be written as

$$BER = \Pr(\text{off})\Pr(\text{on}|\text{off}) + \Pr(\text{on})\Pr(\text{off}|\text{on}) \tag{26}$$

where $\Pr(\text{on})$ and $\Pr(\text{off})$ are the probabilities of sending "on" and "off" bits, respectively. Because the transmitted signal is taken as symbols drawn equiprobably, thus $\Pr(\text{on}) = \Pr(\text{off}) = 0.5$. $Pr(\text{on}|\text{off})$ and $Pr(\text{off}|\text{on})$ are the conditional bit error probabilities when the transmitted bit is "off" and "on," respectively.

According to Eq. (8), $\Pr(\text{off}|\text{on})$ can be written as

$$\begin{aligned} \Pr(\text{off}|\text{on}) &= \Pr(y < \xi P|\text{on}) \\ &= \int_{-\infty}^{\xi P} \frac{1}{\sqrt{2\pi(1 + 2\xi P\varsigma^2)}\sigma} e^{-\frac{(y-2\xi P)^2}{2(1+2\xi P\varsigma^2)\sigma^2}} \mathrm{d}y \\ &= \mathcal{Q}\left(\frac{\xi P}{\sqrt{1 + 2\xi P\varsigma^2}\sigma}\right) \end{aligned} \tag{27}$$

where $\mathcal{Q}(x)$ is the Gaussian Q-function.

Moreover, $\Pr(\text{off}|\text{on})$ can be similarly written as

$$\begin{aligned}\Pr(\text{off}|\text{on}) &= \Pr(y > \xi P|\text{off}) \\ &= \int_{\xi P}^{\infty} \frac{1}{\sqrt{2\pi}\sigma} e^{-\frac{y^2}{2\sigma^2}} \mathrm{d}y \\ &= \mathcal{Q}\left(\frac{\xi P}{\sigma}\right).\end{aligned} \tag{28}$$

Therefore, the BER can be finally written as

$$BER = \frac{1}{2}\left[\mathcal{Q}\left(\frac{\xi P}{\sqrt{1+2\xi P\varsigma^2}\sigma}\right) + \mathcal{Q}\left(\frac{\xi P}{\sigma}\right)\right]. \tag{29}$$

Remark 6: Let the average SNR be $\gamma = \xi P/[(1+\xi P\varsigma^2)\sigma^2]$. Because ξ, P and ς are non-negative and finite numbers, $\gamma \to \infty$ (or 0) is equivalent to $\sigma^2 \to 0$ (or ∞). Apparently, BER in Eq. (29) is a monotonic decreasing function with respect to γ. Therefore, we have

$$\lim_{\gamma\to\infty} BER = 0 \tag{30}$$

$$\lim_{\gamma\to 0} BER = \frac{1}{2} \tag{31}$$

This indicates that the minimum BER and the maximum BER are 0 and 0.5, respectively.

Remark 7: When $\varsigma = 0$, BER can be simplified as

$$BER|_{\varsigma=0} = \mathcal{Q}\left(\frac{\xi P}{\sigma}\right). \tag{32}$$

5. Numerical results

In this section, some classical numerical results will be presented. The derived theoretical expressions of the mutual information, the lower bound of mutual information and the BER will be verified.

5.1. Results of mutual information

Figure 3 shows the mutual information (i.e., $I(X;Y)$ in Eq. (12)) and its lower bound (i.e., $I_{\text{Low}}(X;Y)$ in Eq. (19)) versus SNR with different modulation orders N. In the simulation, without loss of generality, ξ, P and ς are set to be one. In **Figure 3**, it can be seen that $I(X;Y)$ and $I_{\text{Low}}(X;Y)$ are monotonic increasing functions with respect to SNR. Moreover, with the increase of N, $I(X;Y)$ and $I_{\text{Low}}(X;Y)$ also increase. It can also be found that the maximum value of $I(X;Y)$ is $\log_2 N$, and the maximum value of $I_{\text{Low}}(X;Y)$ is $\log_2 N - \log_2(e)/2 - 1/2$, which coincides with *Remark 1*. Furthermore, the gap between $I(X;Y)$ and $I_{\text{Low}}(X;Y)$ is $(\log_2 e - 1)/2$ bits at low and high SNR regions, which coincides with *Remark 4*.

Figure 4 shows the mutual information (i.e., $I(X;Y)$ in Eq. (12)) and its lower bound (i.e., $I_{\text{Low}}(X;Y)$ in Eq. (19)) versus dimming targets ξ with different ς. In the simulation, P is set to be one, $\gamma = 20$dB and $N = 4$.As can be seen, when $\varsigma = 1$ and $\varsigma = 10$, $I(X;Y)$ and $I_{\text{Low}}(X;Y)$ increase with the increase of ξ, while $I(X;Y)$ and $I_{\text{Low}}(X;Y)$ do not change with the increase of ξ when $\varsigma = 0$. Moreover, it can be seen that $I(X;Y)$ and $I_{\text{Low}}(X;Y)$ are both the monotonic increasing functions with respect to ς.

http://dx.doi.org/10.5772/68019

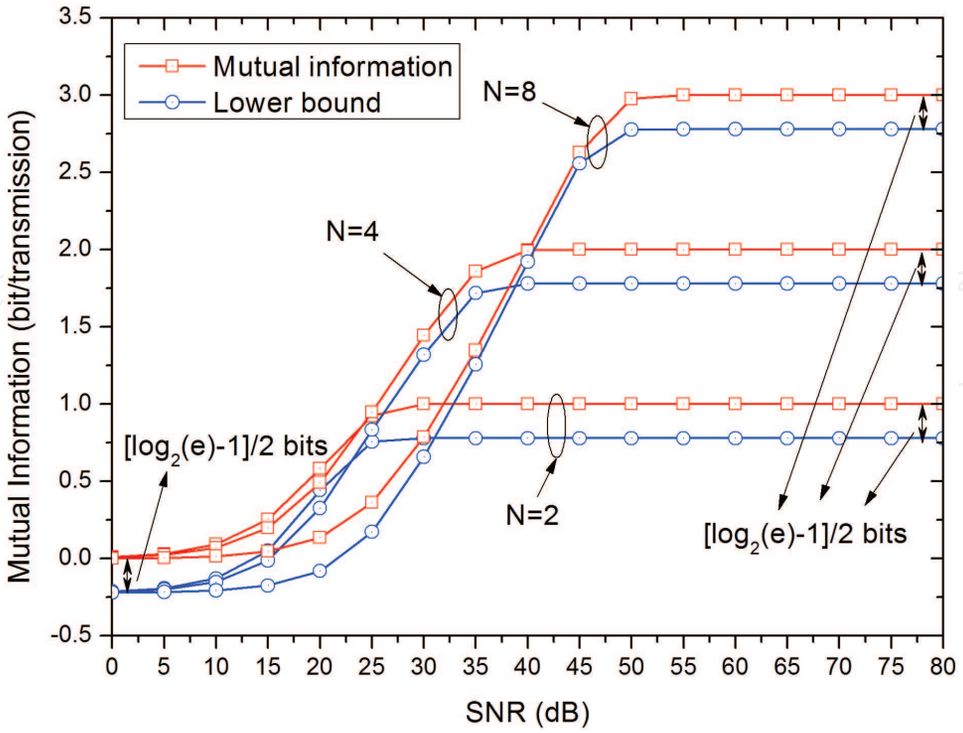

Figure 3. Mutual information and its lower bound versus SNR with different N.

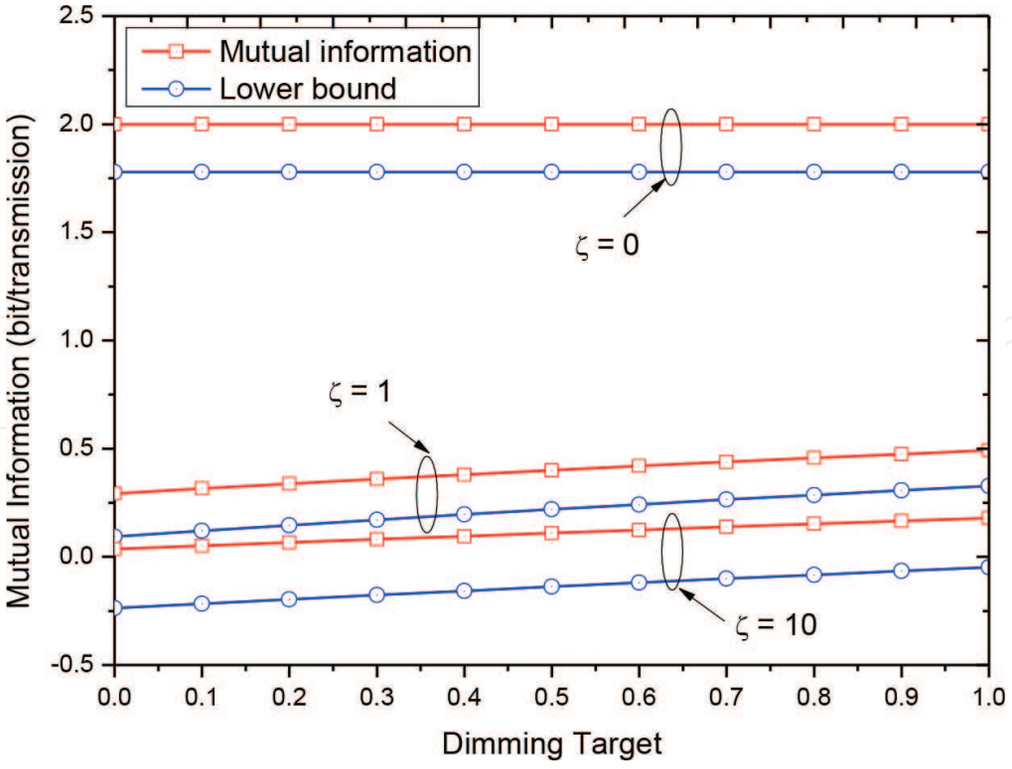

Figure 4. Mutual information and its lower bound versus dimming target ξ with different ς.

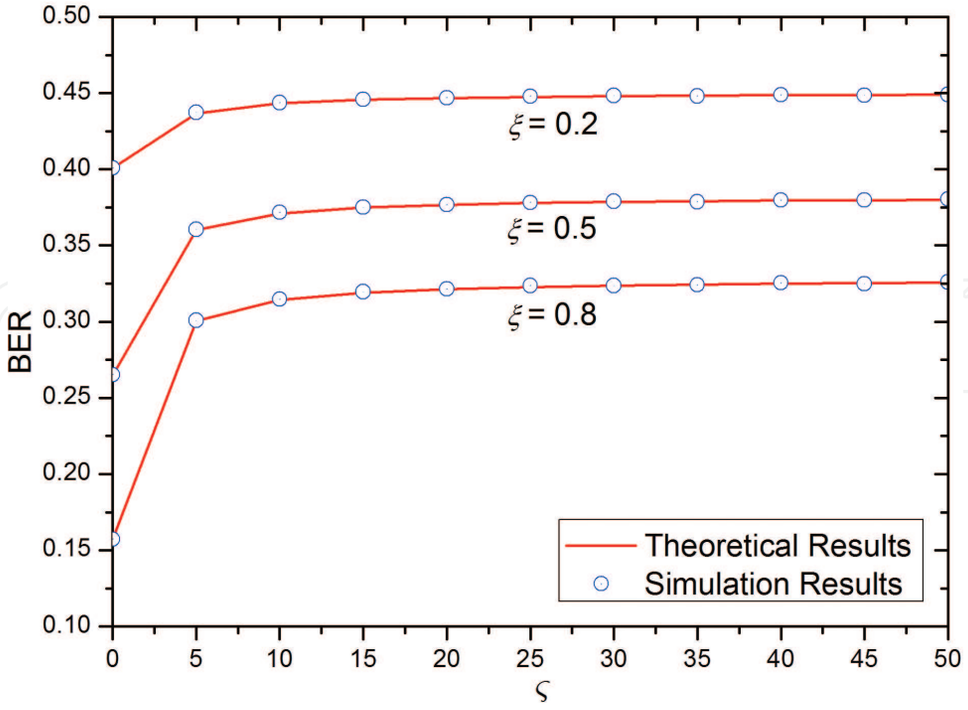

Figure 5. BER versus ς with different ξ.

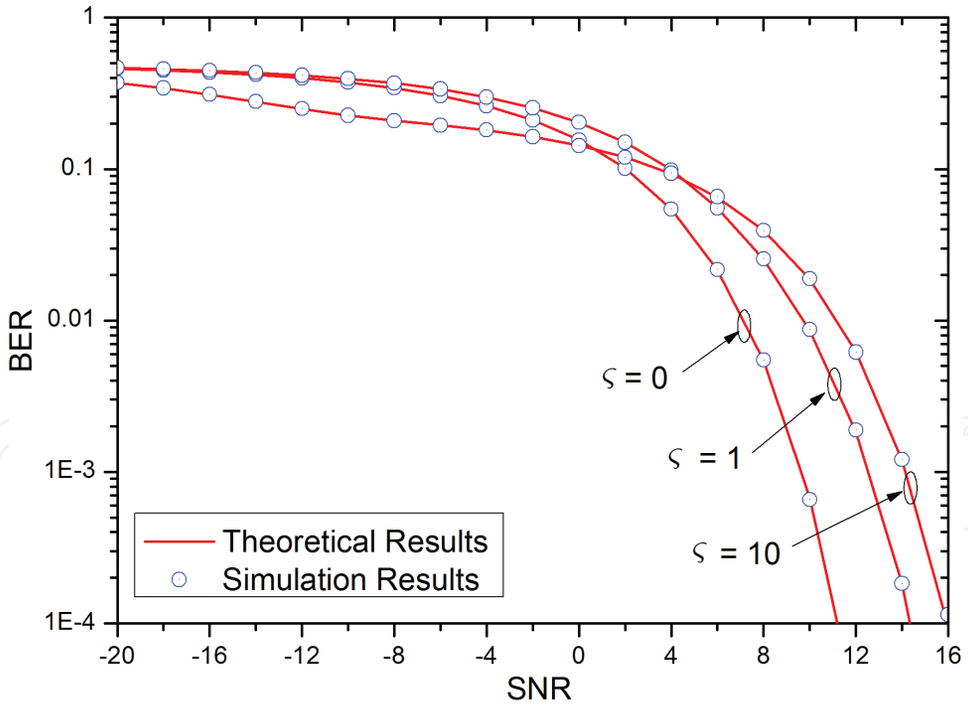

Figure 6. BER versus SNR with different ς.

5.2. Results of BER

Figure 5 shows BER versus ς with different dimming targets ξ. In the simulation, both P and σ are set to be one. It can be seen that the best BER performance is achieved when $\varsigma = 0$, which

indicates that the performance for the system with only input-independent noise outperforms that with input-dependent noise. Moreover, with the increase of ς, the BER performance degrades. Furthermore, it can be observed that with the increase of ξ, the value of the BER reduces, which indicates that the system performance improves. In addition, it can be found that the theoretical results show close agreement with the Monte-Carlo simulation results, which verifies the correctness of the derived theoretical expression of the BER.

Figure 6 shows the BER versus the SNR with different ς. It can be observed that the value of the BER decreases with the increase of the SNR. This is because large SNR will generate a small BER, and thus it will result in good performance. Moreover, at low SNR region, the curve with $\varsigma = 10$ achieves the best BER performance. At high SNR region, the curve with $\varsigma = 0$ achieves the best BER performance. Once again, the gap between the theoretical results and the simulation results is so small enough to be ignored, which verifies the accuracy of the derived theoretical expression of the BER.

6. Conclusions

This chapter investigates the performance of the VLC with input-dependent noise. The theoretical expression of the mutual information is derived, which is not in a closed form. Moreover, the closed-form expression of the lower bound on the mutual information is obtained. Furthermore, by employing the OOK, the theoretical expression of the BER for the VLC is derived. Numerical results show that the derived theoretical expressions in this chapter are quite accurate to evaluate the system performance without time-intensive simulations.

Acknowledgements

This work is supported by National Natural Science Foundation of China (61571115, 61372106, 61223001, 61322112, 61401399, and 61531166004), Research Project (2014CB360507), the open research fund of National Mobile Communications Research Laboratory, Southeast University (2017D06), and NUPTSF (NY216009).

Author details

Jin-Yuan Wang[1,2]*, Jun-Bo Wang[2] and Yongjin Wang[1]

*Address all correspondence to: jywang@njupt.edu.cn

1 Peter Grünberg Research Centre, Nanjing University of Posts and Telecommunications, China

2 National Mobile Communications Research Laboratory, Southeast University, China

References

[1] A. Jovicic, J. Li, T. Richardson. Visible light communication: opportunities, challenges and the path to market. IEEE Communications Magazine. 2013;**51**(12):26–32. doi:10.1109/MCOM.2013.6685754

[2] J. Armstrong, Y. A. Sekercioglu, A. Neild. Visible light positioning: a roadmap for international standardization. IEEE Communications Magazine. 2013;**51**(12):68–73. doi:10.1109/MCOM.2013.6685759

[3] L. Zeng, D. C. O'Brien, H. L. Minh, G. E. Faulkner, K. Lee, D. Jung, Y. J. Oh, T. Won. High data rate multiple input multiple output (MIMO) optical wireless communications using white led lighting. IEEE Journal on Selected Areas in Communications, 2009;**27**(9):1654–1662. doi:10.1109/JSAC.2009.091215

[4] K.-I. Ahn, J. K. Kwon. Capacity analysis of M-PAM inverse source coding in visible light communications. Journal of Lightwave Technology. 2012;**30**(10):1399–1404. doi:10.1109/JLT.2012.2185780

[5] J.-B. Wang, Q.-S. Hu, J. Wang, M. Chen, J.-Y. Wang. Tight bound on channel capacity for dimmable visible light communications. IEEE/OSA Journal of Lightwave Technology. 2013;**31**(23):3771–3779. doi:10.1109/JLT.2013.2286088

[6] R. Jiang, Z. Wang, Q. Wang, L. Dai. A tight upper bound on channel capacity for visible light communications. IEEE Communications Letters. 2016;**20**(1):97–100. doi:10.1109/LCOMM.2015.2497694

[7] J.-B. Wang, Q.-S. Hu, J. Wang, M. Chen, Y.-H. Huang, J.-Y. Wang. Capacity analysis for dimmable visible light communications. In: IEEE International Conference on Communications, June, 2014, Sydney. IEEE; 2014, pp. 3331–3335. doi:10.1109/ICC.2014.6883835

[8] J.-Y. Wang, J. Dai, R. Guan, L. Jia, Y. Wang, M. Chen. On the channel capacity and receiver deployment optimization for multi-input multi-output visible light communications. Optics Express. 2016;**24**(12):13060–13074. doi:10.1364/OE.24.013060

[9] A. Chaaban, Z. Rezki, M.-S. Alouini. Fundamental limits of parallel optical wireless channels: capacity results and outage formulation. IEEE Transactions on Communications. 2016;**65**(1):296–311. doi:10.1109/TCOMM.2016.2621743

[10] A. Chaaban, Z. Rezki, M.-S. Alouini. Low-SNR capacity of parallel IM-DD optical wireless channels. IEEE Communications Letters. LCOMM.2016.2633339

[11] J. Grubor, S. Randel, K.-D. Langer, J. Walewski. Broadband information broadcasting using LED-based interior lighting. IEEE/OSA Journal of Lightwave Technology. 2008;**26**(24):3883–3892. doi:10.1109/JLT.2008.928525

[12] L. Hanzo, H. Haas, S. Imre, D. O'Brien, M. Rupp, L. Gyongyosi. Wireless myths, realities, and futures: from 3G/4G to optical and quantum wireless. Proceedings of the IEEE. 2012;**100**(Special Centennial Issue):1853–1888. doi:10.1109/JPROC.2012.2189788

[13] S. M. Moser. Capacity results of an optical intensity channel with input-dependent Gaussian noise. IEEE Transactions on Information Theory. 2012;**58**(1):207–223. doi:10.1109/TIT.2011.2169541

[14] A. Lapidoth, S. M. Moser, M. A. Wigger. On the capacity of free-space optical intensity channels. IEEE Transactions on Information Theory. 2009;**55**(10):4449–4461. doi:10.1109/TIT.2009.2027522

[15] T. Komine, M. Nakagawa. Fundamental analysis for visible-light communication system using LED lights. IEEE Transactions on Consumer Electronics. 2004;**50**(1):100–107. doi:10.1109/TCE.2004.1277847

[16] J.-Y. Wang, Z. Yang, Y. Wang, M. Chen. On the performance of spatial modulation-based optical wireless communications. IEEE Photonics Technology Letters. 200916;**28**(19):2094–2097. doi:10.1109/LPT.2016.2585502

[17] J. M. Kahn, J. R. Barry. Wireless infrared communications. Proceedings of the IEEE. 1997;**85**(2):265–298. doi:10.1109/5.554222

[18] J.-B. Wang, Q.-S. Hu, J. Wang, Y.-H. Huang, J.-Y. Wang. Channel capacity for dimmable visible light communications. In: IEEE Global Communications Conference, December 2013, Atlanta. IEEE; 2013, pp. 2424–2429. doi:10.1109/GLOCOM.2013.6831437

[19] J.-Y. Wang, J.-B. Wang, M. Chen, J. Wang. Capacity bounds for dimmable visible light communications using PIN photodiodes with input-dependent Gaussian noise. In: IEEE Global Communications Conference; 8–12 December 2014; Austin, TX. IEEE; 2014, pp. 2107–2112. doi:10.1109/GLOCOM.2014.7037112

IntechOpen